

System optimal dynamic lane reversal for autonomous vehicles

Melissa Duell¹(corresponding), Michael W. Levin², Stephen D. Boyles², S. Travis Waller¹

¹School of Civil and Environmental Engineering
University of New South Wales, Sydney, Australia

²Department of Civil, Architectural, and Environmental Engineering
The University of Texas at Austin, Austin, United States

Corresponding author: m.duell@unsw.edu.au

Abstract—Transformative technologies such as autonomous vehicles (AVs) create an opportunity to reinvent features of the traffic network to improve efficiency. The focus of this work is dynamic lane reversal: using AV communications and behavior to change the direction vehicles are allowed to travel on a road lane with much greater frequency than would be possible with human drivers. This work presents a novel methodology based on the linear programming formulation of dynamic traffic assignment using the cell transmission model for solving the system optimal (SO) problem. The SO assignment is chosen because the communications and behavior protocols necessary to operate AV intersection and lane reversal controls could be used to assign routes and optimize network performance. This work expands the model to determine the optimal direction of lanes at small space-time intervals. Model assumptions are outlined and discussed. Results demonstrate the model and explore the dynamic demand scenarios which are most conducive to increasing system efficiency with dynamic lane reversal.

Keywords—dynamic lane reversal; autonomous vehicles; dynamic traffic assignment; system optimal

I. INTRODUCTION

Technological advances in autonomous vehicles (AVs) introduce the possibility of new communication and behavior protocols that could significantly improve traffic efficiency. For example, researchers have shown that the reservation-based control [1] reduces intersection delays under a variety of traffic demand scenarios [2]. Another proposed protocol with great potential, and the focus of the current work, is *dynamic lane reversal* (DLR), which can be described as frequent changes to the direction vehicles are permitted to travel on a lane in response to dynamic traffic conditions.

The concept of DLR stems from contraflow lanes used in evacuation scenarios and reversible lanes which are used to alleviate peak hour congestion in many locations. One example is the Sydney Harbour Bridge, which has eight lanes, of which three change direction daily for morning and evening peak traffic. The greatest challenge for contraflow lanes that limits the timeframe of application is the reaction of human drivers. Drivers who do not respond appropriately will at best negate the benefits, and at worse could cause a head-on collision. Consequently, rapid direction changes are not available for contraflow lanes.

Most previous work focuses on evacuation (for instance, see [3]; [4]; [5]), although some literature addresses contraflow lanes for peak hour demand. Zhou et al. [6] and Xue and Dong [7] use machine learning techniques to decide when to use contraflow for a bottleneck link. Meng et al. [8] use a bi-level formulation, with traffic assignment as the subproblem, because the driver response to contraflow lanes results affects the user equilibrium (UE).

To address the limitations of contraflow lanes, Hausknecht et al. [9] proposed DLR for AVs. They studied two models: first, DLR in a micro-simulation with lane direction decided by road saturation; and second, a bi-level problem for deciding lane direction in static flow context with traffic assignment as the subproblem. However, both of these models focused on stationary demand. The goal of this paper therefore is to develop a DLR model responsive to time-varying demand. In scenarios such as a congested downtown grid, different directions may become oversaturated at different times in the AM or PM peak. Depending on network topology, demand does not necessarily prefer a single direction. These conditions warrant a more adaptive policy to dynamic lane reversal as well as an aggregate but dynamic flow model for studying larger networks.

To address these objectives, this paper uses the cell transmission model (CTM) proposed by Daganzo [10], [11]. CTM is frequently applied in dynamic traffic assignment (DTA) models. CTM captures traffic waves while being computationally tractable for larger networks. It also admits space-time dependent fundamental diagrams, which are necessary for modeling DLR. Because efficiency may be improved by partial lane reversal, such as through a temporary turning bay, lane reversal is decided at the cell level.

Because UE behavior can be a significant obstacle to improving system efficiency, as demonstrated by the Braess paradox [12], we assume that route choice is assigned by a system manager resulting in system optimal (SO) conditions. For AVs in communication with intersection managers to facilitate intersection reservations and DLR, it is feasible for AVs to follow assigned routes. In a future where all vehicles are autonomous, policymakers may require vehicles to follow SO routes. UE behavior also makes the problem more

complex: to find the optimal DLR policy when vehicles route themselves requires solving DTA as a subproblem to DLR. Therefore, this work focuses on the SO version of the problem.

The contributions of this paper are summarized by the following:

- We develop a system optimal dynamic traffic assignment model incorporating dynamic lane reversal (DLR-SODTA) in order to demonstrate the potential and feasibility of DLR
- We formulate the model using a mixed integer linear program (MILP) based on a well-established SODTA model [13]. This application solves the optimization problem for lane allocation as part of the combined DLR and SO assignment problem.
- We use this model to find the optimal lane allocation at different times for varying demand scenarios and compare these results with the fixed lane scenario.

The remainder of this paper is organized as follows. Section II introduces the DLR constraints and decision variables to develop the MILP model. Section III presents the potential improvement on a bottleneck link with varying demand. Conclusions are discussed in Section IV.

II. METHODOLOGY

A. Assumptions

AV behavior using current road technology has yet to be well-defined. Additionally, behaviors using proposed technologies that exist only in concept such as reservation-based intersections or DLR are even less established. Therefore, we make the following assumptions about vehicle behavior in this model:

1) *All vehicles are AVs.* The additional complexities of DLR with human drivers are outside the scope of this paper and will be explored in future work.

2) *SO behavior.* As mentioned previously, AVs already follow substantial communications and behavior protocols. They may also be required to follow an assigned route in order to optimize system performance in a previously unachievable manner. This assumption is beneficial because it implies that the locations of vehicles in the network can be predicted and the lane configuration can be solved as an optimization problem. The UE assumption presents a greater challenge that will be the subject of future work.

3) *Required lane changing.* We assume that vehicles may be required to change lanes up to κ times per timestep. For example, a common CTM timestep of 6 seconds with free flow speed of 48 km per hour results in a cell length of 80 m. Thus, a 6 second timestep should be sufficient for at least one lane change.

4) *Perfect information of demand.* Finding the SO assignment requires some knowledge of future demand. We assume demand is known perfectly. This is reasonable for peak hours, during which DLR has the greatest potential to reduce congestion. During peak hours, the departure time for

travelers leaving home for work, or leaving work for home, is fairly consistent, and the origin/destination may be specified in advance. Additionally, a centralized network manager may log vehicle travel in a consistent manner to predict demand.

For simplicity of modeling lane changing and turning movement behavior, we model all lanes in one direction as being contiguous. Therefore, the lane direction problem reduces to specifying the number of lanes in each direction for each pair of cells. For any link $[a, b]$, we say it is *paired* with link $[b, a]$ if $[a, b]$ and $[b, a]$ have the same length and free flow speed. This would result in each link in the pair having the same number of cells, with each cell $i \in [a, b]$ having a corresponding cell $\tilde{i} \in [b, a]$ in the opposite direction. Establishing the pairing of cells and links is necessary to determine the number of lanes available for allocation.

B. Formulation

The MILP is based on the SO linear program (LP) for CTM by Ziliaskopoulos [14] for a single destination and Li et al. (2003) for more general networks. The SODTA formulation by Ziliaskopoulos has been widely applied in a number of research applications [15]. CTM more realistically propagates traffic than alternative approaches relying on link performance functions. It faces challenges due to the size of the linear program, the “holding back” phenomenon [16], and in multi-destination applications, FIFO violations [17]. While addressing these issues is beyond the scope of the current work, it is possible that in a network comprised solely of AVs, the latter two could represent realistic behavior.

The addition of the number of lanes per cell, assumed to be integer, requires an MILP as opposed to an LP. In preparation for the formulation, let C be the set of cells and E the set of cell connectors. Let $C_R \subset C$ and $C_S \subset C$ be the sets of origin and destination cells, respectively. Let T be the set of discrete time intervals. Without loss of generality, and for simplicity of notation, let the timestep be 1. To define cell transitions, let $\Gamma^-(i)$ and $\Gamma^+(i)$ be the sets of preceding and succeeding cells to cell i . For the fundamental diagram, let N_i^t be the maximum number of vehicles that can fit in cell i per lane at time t and let Q_i^t be the capacity per lane for cell i at time t . As with Daganzo’s [10] CTM, this model uses the trapezoidal fundamental diagram $\Psi_i^t(x) = \min\{x, Q_i^t, w(N_i - x)\}$, where w is backwards wave speed. Let d_{rs}^t be the demand for $(r, s) \in C_R \times C_S$ at time t . Let P be a set of all pairs of corresponding cells (a, b) .

The decision variables are cell density $x_{rs,i}^t$, cell transition flows $y_{rs,ij}^t$ from $i \in C$ to $j \in C$ per origin-destination pair (r, s) at time t , and the number of lanes per cell l_i^t . Including the number of lanes as a decision variable is one of the advantages of this model.

The objective of the DLR-SODTA model is to minimize total system travel time, which due to the CTM assumptions, is simply the summation of the density of each cell over all time steps. This results in the following MILP:

$$\min Z = \sum_{(r,s) \in C_R \times C_S} \sum_{t \in T} \sum_{i \in C \setminus C_S} x_{rs,i}^t \quad (1)$$

s.t.

$$x_{rs,j}^{t+1} = x_{rs,j}^t + \sum_{i \in \Gamma^-(j)} y_{rs,ij}^t - \sum_{k \in \Gamma^+(j)} y_{rs,jk}^t \quad \begin{matrix} \forall_{(r,s) \in C_R \times C_S}, \\ \forall_{j \in C \setminus (C_R \cup C_S)}, \\ \forall_{t \in T} \end{matrix} \quad (2)$$

$$x_{rs,j}^{t+1} = x_{rs,j}^t + \sum_{i \in \Gamma^-(j)} y_{rs,ij}^t \quad \begin{matrix} \forall_{(r,s) \in C_R \times C_S}, \\ \forall_{j \in C_S}, \\ \forall_{t \in T} \end{matrix} \quad (3)$$

$$\sum_{j \in \Gamma^+(i)} y_{rs,ij}^t \leq x_{rs,i}^t \quad \begin{matrix} \forall_{(r,s) \in C_R \times C_S}, \\ \forall_{i \in C \setminus (C_R \cup C_S)}, \\ \forall_{t \in T} \end{matrix} \quad (4)$$

$$\sum_{\forall r \in C_R} \sum_{\forall s \in C_S} (\sum_{i \in \Gamma^-(j)} y_{rs,ij}^t + \delta x_{rs,j}^t) \leq \delta N_j l_j^t \quad \begin{matrix} \forall_{j \in C \setminus (C_R \cup C_S)}, \\ \forall_{t \in T} \end{matrix} \quad (5)$$

$$\sum_{\forall r \in C_R} \sum_{\forall s \in C_S} \sum_{\forall i \in \Gamma^-(j)} y_{rs,ij}^t \leq Q_j^t l_j^t \quad \begin{matrix} \forall_{j \in C \setminus (C_R \cup C_S)}, \\ \forall_{t \in T} \end{matrix} \quad (6)$$

$$\sum_{\forall r \in C_R} \sum_{\forall s \in C_S} \sum_{\forall j \in \Gamma^+(i)} y_{rs,ij}^t \leq Q_i^t l_i^t \quad \begin{matrix} \forall_{i \in C \setminus (C_R \cup C_S)}, \\ \forall_{t \in T} \end{matrix} \quad (7)$$

$$x_{rs,r}^{t+1} - x_{rs,r}^t + \sum_{j \in \Gamma^+(r)} y_{rs,rj}^t = d_{rs}^t \quad \begin{matrix} \forall_{(r,s) \in C_R \times C_S}, \\ \forall_{r \in C_R}, \\ \forall_{t \in T} \end{matrix} \quad (8)$$

$$x_{rs,i}^0 = 0, y_{rs,ij}^0 = 0 \quad \begin{matrix} \forall_{(r,s) \in C_R \times C_S}, \\ \forall_{(i,j) \in E}, \\ \forall_{t \in T} \end{matrix} \quad (9)$$

$$y_{rs,ij}^t \geq 0 \quad \begin{matrix} \forall_{(r,s) \in C_R \times C_S}, \\ \forall_{(i,j) \in E}, \\ \forall_{t \in T} \end{matrix} \quad (10)$$

$$l_i^{t+1} \leq l_i^t + \kappa \quad \forall_{i \in C} \forall_{t \in T} \quad (11)$$

$$l_i^{t+1} \geq l_i^t - \kappa \quad \forall_{i \in C} \forall_{t \in T} \quad (12)$$

$$l_a^t + l_b^t = L_{ab} \quad \forall_{(a,b) \in E} \quad (13)$$

$$l_i^t \geq 0 \quad \forall_{i \in C} \forall_{t \in T} \quad (14)$$

where δ is the ratio of backwards wave speed to free flow speed. Constraints (2) through (9) define the cell transition flows. Constraints (5), (6), and (7) have been modified from the original multi-destination CTM linear programming model to account for the explicit representation of multiple lanes as a decision variable. Constraints (11) and (12) place a bound on the number of lanes that can be reversed per time period, and constraint (14) defines the number of lanes available to any pair of cells as L_{ab} , the total number of lanes available to both cells, which is an input to the model. Note that all available lanes must be allocated during all time periods, which will at times results in an arbitrary lane configuration.

C. Analysis

Let Z^* be the optimal value of the objective function. Also, let $\bar{Z} = Z$ solved with the additional constraints

$$l_i^t = \bar{l}_i \quad \forall_{i \in C} \forall_{t \in T} \quad (16)$$

for some \bar{l}_i 's satisfying $\bar{l}_a + \bar{l}_b \leq L_{ab}$ and $l_i \geq 0 \forall_{i \in C}$. Let \bar{Z}^* be the optimal solution with corresponding flow and lane assignment (\bar{y}^*, \bar{l}) . \bar{Z}^* reduces to solving the SO problem with a fixed lane configuration \bar{l} . Clearly, (\bar{y}^*, \bar{l}) is a feasible solution to the original problem since the fixed configuration constraint (14) satisfies constraints (11) through (13). This results in the following proposition:

Proposition 1. $Z^* \leq \bar{Z}^*$.

III. DEMONSTRATION AND ANALYSIS

This section presents the DLR-SODTA model results on a small corridor example. The DLR results are compared with the fixed-lane results. The DLR-SODTA problem was solved using the AMPL programming interface to the CPLEX solver.

A. Network description

The DLA-SODTA model is initially demonstrated on a simple two-link example in order to closely analyze the relationship between dynamic lane allocation and dynamic traffic demand patterns. Both links are of length 650 m with a free flow speed of 50 kph. Each link has two lanes with a capacity of 1800 vehicles/hour/lane. Figure 1 illustrates the demonstration network.

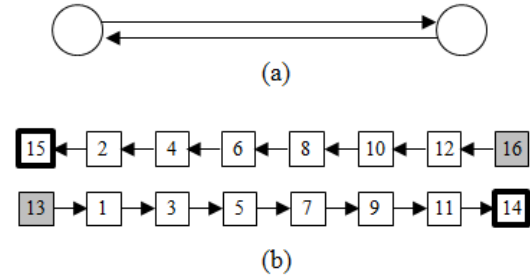


FIGURE 1. (A) SIMPLE TWO LINK NETWORK AND (B) CELL NETWORK REPRESENTATION

Using a time increment of 6 seconds, the each link is comprised of 8 cells with $N_i = 13.2$ vehicles and $Q_i = 3$ vehicles. In all cases, κ , the number of lanes which may change direction during a time period, is 1. We examine four demand cases and compare the DLR and fixed lane SODTA results. Demand case I is illustrated in Figure 2.

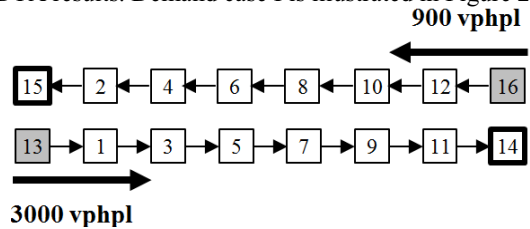


FIGURE 2. DEMAND CASE (I)

In case (I), the vehicle flow is much higher in one direction. In the traditional fixed lane network, this situation will result in congested conditions. The SODTA model considered 30

time steps, or 3 minutes of simulation. Demand for the first ten time steps was assumed to be $d_{13,14}^{0..9} = 10$ vehicles and $d_{16,15}^{0..9} = 3$ vehicles respectively. The demand follows a uniform departure time profile.

The DLR model resulted in a total travel time of 5166 seconds and 18 time increments for all vehicles to exit the network. The fixed-lane approach was higher with a total travel time of 6834 seconds and 23 time-increments for all vehicles to exit.

Figure 3 shows a detailed representation of the lane configuration for pairs of cells. Each vertical column represents the four lanes that are shared by a pair of cells. The green shows that a lane is assigned to the first cell in the pair, while the red represents a lane assignment to the second cell in the pair. For example, under pair (13,15), all four lanes are assigned to cell 13 until time period 7. In demand case I, the vehicle flow was unbalanced and therefore a majority of the lanes were able to be utilized by the direction with a higher volume of flow. Also note that when there is no vehicle demand for the cell or cell connector, the lane is assigned arbitrarily.

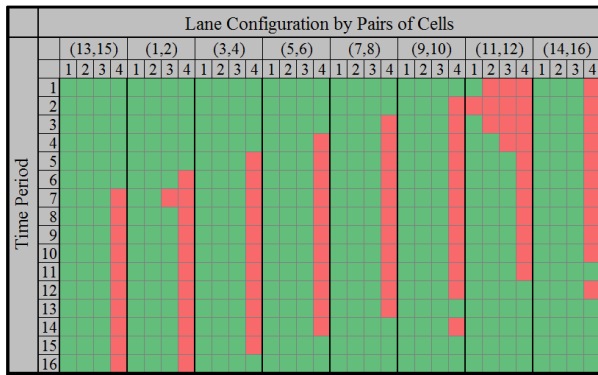


FIGURE 3. LANE CONFIGURATION IN DEMAND CASE (I)

In the second case, the flow from both directions is more equal, as Figure 4 shows. This is a common case for congested network corridors, even during peak hours. Demand for the first ten time steps was assumed to be $d_{13,14}^{0..9} = 9$ vehicles and $d_{16,15}^{0..9} = 5$ vehicles.

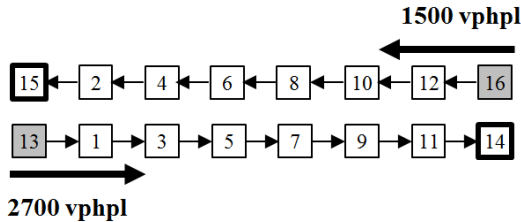


FIGURE 4. BALANCED DEMAND CASE (II-IV)

In the fixed lane case, the model requires 16 time periods for all the flow to exit the network while the DLR model requires 20 time-increments. The total travel time in the fixed case was 7230 seconds and in the DLR case was 6756 seconds. Again, the DLR model was able to reduce the total

travel time. However, because there were more vehicles from both directions, the reduction was not as great.

Demand case III examines the impact of time dependent demand, which an important consideration for network operators. In this case, the total vehicle demand is the same (90 vehicles/3 minutes) but the departure times are different. In this scenario, the departure time are more spaced out and we assume $d_{13,14}^{0..4} = 18$ vehicles and $d_{16,15}^{10..14} = 10$ vehicles.

Both the fixed-lane and the DLR models require 25 time periods for all vehicles to exit the network. However, the total travel time in the fixed case was 9084 seconds and in the DLR case was 7488 seconds.

In addition, Figure 5 shows the detailed lane configuration in demand case III. This demand scenario may be particularly conducive to dynamic lane allocation because the first wave of demand from (13,14) had sufficient time to exit the network before the second wave of demand from (16,15) entered the network.

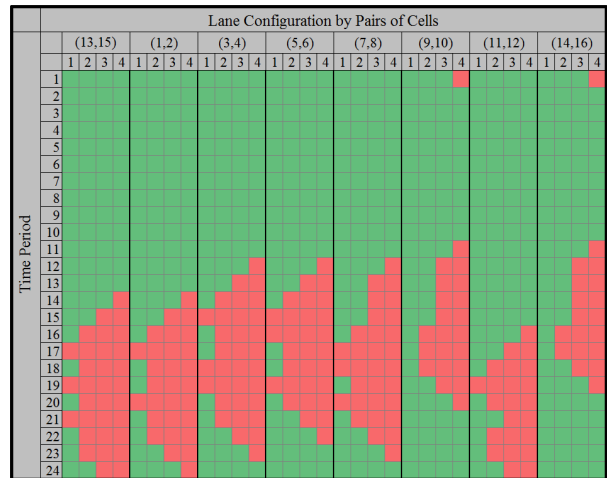


FIGURE 5. LANE CONFIGURATION IN DEMAND CASE (III)

Finally, we examine the “peak” demand case where the total demand at each departure time is no longer uniform.

TABLE 1. PEAK DEPARTURE PATTERN DEMAND

Time Period	(14,13)	(16,15)
0	5	0
1	15	0
2	10	0
3	30	0
4	30	0
5	0	5
6	0	5
7	0	20
8	0	18
9	0	2
Total	90	50

The total travel time for the fixed case is 8958, while the total travel time for the DLR-SODTA is 8718. The vehicles exited the network in 22 time-steps versus 18 time-steps. Table 2 summarizes the results from the four demand cases. Additionally, Table 2 presents the results for the case in which only two of the four lanes are available to change directions as DLR¹. This would ensure that for all time periods, each direction has at least one lane available which could be another possible dynamic lane configuration.

TABLE 2. SUMMARY OF RESULTS

	Total Demand	Departure Profile	# Departure Periods	Fixed (s)	DLR (s)	DLR ¹ (s)
I	100, 30	Uniform	10	7464	5796	5796
II	90, 50	Uniform	10	7230	6756	6756
III	90, 50	Uniform	5	9084	7488	8220
IV	90, 50	Peak	5	8958	8718	8718

Finally, we examined a 30 minute CTM simulation period, which is 300 time steps. We loaded demand at the same rate (9 and 5 vehicles per timestep respectively) for 15 minutes, or 150 time steps. In this case, we placed a constraint that required that there be at least one lane in each direction during all times periods (called DLR¹). There was a total of 1,350 vehicles between (13,14) and 750 between (16,15).

The DLR solution assigned 3 lanes to the direction with a greater volume of vehicles and then switched to a 2 lanes in each direction configuration after 108 time increments. This relatively static assignment of lanes is expected because of the uniform demand profile. If the demand were to arrive in more of a heavy-slow pattern, we would expect there to be more changes in lane configuration as more capacity was switched to the favored direction of travel.

The total travel time in the fixed case was 108.9 hours. The DLR model reduced the travel time to 69.4 hours, which represented 36% of the travel time.

IV. CONCLUSION AND FUTURE DIRECTIONS

The presence of autonomous vehicles will give network operators the chance to increase the efficiency of traffic streams using previously impossible approaches. This work investigates the concept of dynamic lane reversal, where the direction vehicles are allowed to travel on a lane is changed at very short time intervals.

We proposed a mixed integer linear programming model based on a Li et al. (2003)'s model of system optimal dynamic traffic assignment that propagates traffic using the cell transmission model. The number of lanes in each cell is explicitly considered as a decision variable, allowing for real time network design in response to time-varying travel demand. Results illustrate the importance of accounting for time-varying demand profiles when exploring the DLR concept. However, due to the integer representation of lanes, this approach will face significant computation challenges when using traditional optimization techniques. Although the

model presented here supports the possibility of dynamic lane reversal, of course there are still a number of practicalities that were not accounted for, but will be the subject of future research.

As advances in technology make autonomous vehicles an increasingly likely proposition, research exploring their impact on transport planning and operations is of great importance. The issue of dynamic lane reversal and the corresponding network design problem present numerous opportunities. The model proposed here can be improved in the future by addressing some of the known issues with the linear relaxation of the CTM (holding back, FIFO), as well as studying tractable heuristics for large city networks.

REFERENCES

- [1] Dresner, K., & Stone, P. (2006, July). Traffic intersections of the future. In Proceedings of the National Conference on Artificial Intelligence (Vol. 21, No. 2, p. 1593). Menlo Park, CA; Cambridge, MA; London; AAAI Press; MIT Press; 1999.
- [2] Fajardo, D., Au, T. C., Waller, S. T., Stone, P., & Yang, D. (2011). Automated Intersection Control. Transportation Research Record: Journal of the Transportation Research Board, 2259(1), 223-232.
- [3] Zhang, X. M., An, S., & Xie, B. L. (2012, October). A Cell-Based Regional Evacuation Model with Contra-Flow Lane Deployment. In Advanced Engineering Forum (Vol. 5, pp. 20-25).
- [4] Wang, J. W., Wang, H. F., Zhang, W. J., Ip, W. H., & Furuta, K. (2013). Evacuation planning based on the contraflow technique with consideration of evacuation priorities and traffic setup time. Intelligent Transportation Systems, IEEE Transactions on, 14(1), 480-485.
- [5] Dixit, V., & Wolshon, B. (2014). Evacuation traffic dynamics. Transportation research part C: emerging technologies, 49, 114-125. ajandro, D., Au, T. C., Waller, S. T., Stone, P., & Yang, D. (2011). Automated Intersection Control. Transportation Research Record: Journal of the Transportation Research Board, 2259(1), 223-232.
- [6] Zhou, W. W., Livolsi, P., Miska, E., Zhang, H., Wu, J., & Yang, D. (1993, October). An intelligent traffic responsive contraflow lane control system. In Vehicle Navigation and Information Systems Conference, 1993., Proceedings of the IEEE-IEE (pp. 174-181). IEEE.
- [7] Xue, D., & Dong, Z. (2000). An intelligent contraflow control method for real-time optimal traffic scheduling using artificial neural network, fuzzy pattern recognition, and optimization. Control Systems Technology, IEEE Transactions on, 8(1), 183-191.
- [8] Meng, Q., Khoo, H. L., & Cheu, R. L. (2008). Microscopic traffic simulation model-based optimization approach for the contraflow lane configuration problem. Journal of Transportation Engineering, 134(1), 41-49.
- [9] Hausknecht, M., Au, T. C., Stone, P., Fajardo, D., & Waller, T. (2011, October). Dynamic lane reversal in traffic management. In Intelligent Transportation Systems (ITSC), 2011 14th International IEEE Conference on (pp. 1929-1934). IEEE.
- [10] Daganzo, C. F. (1994). The cell transmission model: A dynamic representation of highway traffic consistent with the hydrodynamic theory. Transportation Research Part B: Methodological, 28(4), 269-287.
- [11] Daganzo, C. F. (1995). The cell transmission model, part II: network traffic. Transportation Research Part B: Methodological, 29(2), 79-93.
- [12] Braess, P. D. D. D. (1968). Über ein Paradoxon aus der Verkehrsplanung. Unternehmensforschung, 12(1), 258-268.
- [13] Li, Y., et al. (2003). "A decomposition scheme for system optimal dynamic traffic assignment models." Networks and Spatial Economics 3(4): 441-455.
- [14] Ziliaskopoulos, A. K. (2000). A linear programming model for the single destination system optimum dynamic traffic assignment problem. *Transportation Science*, 34(1), 37-49.

- [15] Shen, W., & Zhang, H. M. (2014). System optimal dynamic traffic assignment: Properties and solution procedures in the case of a many-to-one network. *Transportation Research Part B: Methodological*, 65, 1-17.
- [16] Carey, M., Bar-Gera, H., Watling, D., & Balijepalli, C. (2014). Implementing first-in-first-out in the cell transmission model for networks. *Transportation Research Part B: Methodological*, 65, 105-118.
- [17] Doan, K., & Ukkusuri, S. V. (2012). On the holding-back problem in the cell transmission based dynamic traffic assignment models. *Transportation Research Part B: Methodological*, 46(9), 1218-1238.